Article

Optimal Demand-Side Management Using Flat Pricing Scheme in Smart Grid

Fahad R. Albogamy [1], **Yasir Ashfaq** [2], **Ghulam Hafeez** [3], **Sadia Murawwat** [4], **Sheraz Khan** [2], **Faheem Ali** [5], **Farrukh Aslam Khan** [6] and **Khalid Rehman** [7,*]

[1] Computer Sciences Program, Turabah University College, Taif University, P.O. Box 11099, Taif 26571, Saudi Arabia; f.alhammdani@tu.edu.sa

[2] Department of Electrical Engineering, University of Engineering and Technology, Mardan 23200, Pakistan; yasir.ashfaq135@gmail.com (Y.A.); sheraz@uetmardan.edu.pk (S.K.)

[3] Centre of Renewable Energy, Government Advance Technical Training Centre, Hayatabad, Peshawar 25100, Pakistan; ghulamhafeez393@gmail.com

[4] Department of Electrical Engineering, Lahore College for Women University, Lahore 51000, Pakistan; sadia.murawwat@lcwu.edu.pk

[5] Department of Electrical Engineering, University of Engineering and Technology, Peshawar 25000, Pakistan; faheem@uetpeshawar.edu.pk

[6] Center of Excellence in Information Assurance, King Saud University, Riyadh 11653, Saudi Arabia; fakhan@ksu.edu.sa

[7] Department of Electrical Engineering, CECOS University of IT & Emerging Sciences, Hayatabad, Peshawar 25100, Pakistan

* Correspondence: khalid@cecos.edu.pk; Tel.: +92-300-5976576

Abstract: This work proposes a framework to solve demand-side management (DSM) problem by systematically scheduling energy consumption using flat pricing scheme (FPS) in smart grid (SG). The framework includes microgrid with renewable energy sources (solar and wind), energy storage systems, electric vehicles (EVs), and building appliances like time flexible, power flexible, and base/critical appliances. For the proposed framework, we develop an ant colony optimization (ACO) algorithm, which efficiently schedules smart appliances, and EVs batteries charging/discharging with microgrid and without (W/O) microgrid under FPS to minimize energy cost, carbon emission, and peak to average ratio (PAR). An integrated technique of enhanced differential evolution (EDE) algorithm and artificial neural network (ANN) is devised to predict solar irradiance and wind speed for accurate microgrid energy estimation. To endorse the applicability of the proposed framework, simulations are conducted. Moreover, the proposed framework based on the ACO algorithm is compared to mixed-integer linear programming (MILP) and W/O scheduling energy management frameworks in terms of energy cost, carbon emission, and PAR. The developed ACO algorithm reduces energy cost, PAR, and carbon emission by 23.69%, 26.20%, and 15.35% in scenario I, and 25.09%, 31.45%, and 18.50% in scenario II, respectively, as compared to W/O scheduling case. The results affirm the applicability of the proposed framework in aspects of the desired objectives.

Keywords: scheduling; energy forecasting; artificial neural network; energy management; microgrid generation; EVs; batteries

1. Introduction

Due to the exponential rise in population and economic growth, the dependence on electricity rises, causing hike in the energy consumption. On the record, energy sector's electricity demand has been increased to 45%, and residential and commercial sector's electricity demand will rise to 30% in 2025 [1]. The traditional power grid is inefficient in meeting this rising energy demand due to the outdated infrastructure, lacking bi-directional communication and power flow and a demand response (DR) program. Thus, a power grid emerged with advanced/modern infrastructure as a solution, namely smart grid (SG),

which is a combination of the conventional grid and information and communication technology (ICT). The SG with modern infrastructure accommodates renewable and hybrid generation with controlled two-way power and communication flow to actively involve consumers in the DR program to meet this rising electricity demand of residential buildings [2]. Besides, to meet this increasing electricity demand with least carbon emissions, the use of Renewable Energy Sources (RESs) emerged as a solution [3]. However, RESs have intermittent and stochastic nature depending on weather conditions. To solve this problem effectively, a reliable, precise, and accurate forecasting model is needed for estimating the generation of RESs [4].

The SG DR program persuades consumers to take part in the energy market via Advanced Metering Infrastructure (AMI) to cope with the rising electricity demand with available power generation. The DR program is of two types: price-based DR and incentive-based DR. The first type of DR is related to indirect load control, where consumers manage their load in response to the DR scheme issued by the utility. In contrast, the other type of DR is related to direct load control, where control is with the utility company to manage the consumer's load with in-advance short notice [5]. Since buildings' electricity consumption is more than 80%, which is a significant portion of net energy consumption; hence, the first program is more suitable, where both consumers and utility actively participate to produce optimal power usage schedule of buildings, which is beneficial for both the parties [6].

On this note, more research work in the literature has been conducted to solve buildings' energy management problem via scheduling building appliances using price-based DR programs through mathematical, stochastic, and control techniques. For instance, in [7], authors proposed the MILP technique for effective energy management to save electricity cost, reduce PAR, and schedule smart appliances and electric vehicles (EVs) charging/discharging. Authors in [8] formulated the unit commitment problem and developed Mixed-Integer Non-Linear Programming (MINLP) technique to solve the formulated problem. However, the diesel generator is used, releasing carbon footprint to the environment and is not a vital solution. Likewise, stochastic optimization techniques are developed to solve building's energy management problem [9]. For example, in [10], the authors developed a framework where RESs are integrated with buildings for Demand-Side Management (DSM). The developed framework is based on stochastic optimization to solve problems of DSM to achieve minimum energy cost, energy consumption, and user discomfort. However, PAR is not considered, which is closely related to energy cost minimization. Similarly, control techniques are used to solve buildings' energy management problem. For instance, super twisting sliding mode controller is developed to solve the energy balancing problem in SG [11]. However, key objectives like energy cost, user comfort, carbon emission, and PAR are not catered. The complete literature review is conducted in Section 2.

The discussed models are remarkable contributions to solve the DSM problem of buildings integrated with RESs. However, these models have several demerits. For example, mathematical technique-based models cannot handle nonlinear and stochastic effects, load scheduling in unfeasible hours, and dimensionality problem. Also, mathematical techniques have high complexity and spend more time in reaching the optimal solution. Likewise, stochastic technique-based models have premature convergence problems that lose population diversity, parameters adjustment, and termination criteria. In addition, the mentioned works either considered energy cost or PAR or carbon emission. The above works do not address all objectives simultaneously. Hence, a model is required which solves the intermittency problem of RESs and the DSM problem of buildings integrated with RESs.

With this motivation, in this work, a forecasting model based on Enhanced Differential Evolution (EDE) and Artificial Neural Network (ANN), namely, ANN-EDE, is introduced for accurate microgrid energy generation estimation to solve the intermittency problem of RESs. Then, we develop an Ant Colony Optimization (ACO) algorithm for the proposed framework to solve the DSM problem using FPS by minimizing energy cost, peak

energy consumption, and carbon emission. The novelty and contributions of this work are as follows:

- A framework is developed considering FPS to schedule residential building appliances and charging/discharging of EVs/batteries for solving the DSM problem optimally.
- The ANN-EDE prediction model is developed to estimate microgrid energy generation.
- The ACO algorithm is developed for the proposed framework for power usage and EVs/batteries charging/discharging scheduling using FPS in the presence of user constraints, priority, and utility energy constraints.
- The proposed framework is evaluated by comparing it with MILP based framework and without (W/O) scheduling case in terms of energy cost, carbon emission, and PAR for two scenarios: with microgrid and W/O microgrid.

The rest of this work is organized as follows: The related work is presented in Section 2. The proposed optimal DSM framework is discussed in Section 3. Mathematical modeling and problem formulation is presented in Section 4. Performance evaluation (results and discussion) is demonstrated in Section 5. Finally, this work is concluded in Section 6.

2. Related Work

Before we discuss DSM, price, load, and generation forecasting, some recent work on forecasting is conducted in [12,13]. Various optimization techniques have been developed to solve energy management problems for minimizing energy cost, peak energy consumption, and carbon emission in the literature. In the subsequent subsections, some existing promising techniques like mathematical, stochastic, and control are discussed in detail.

2.1. Mathematical Techniques

Authors in [14–29] developed mathematical techniques to solve energy management problem in SG. In [7], Mixed Integer Linear Programming (MILP) is developed to solve energy management problem for PAR and cost minimization. A game theory model is utilized in [30] to schedule appliances for DSM subjected to energy cost and PAR minimization. However, an important objective is user comfort level, which is not considered. The authors in [31] adopted MILP technique to schedule EVs and load in residential areas for DSM. Authors proposed a novel energy management strategy to operate consumers in various operation modes considering RESs and Energy Storage Systems (ESSs) in smart homes in [32]. The purpose is to achieve objectives like energy cost, peak energy consumption, and pollution emission minimization. In [33], authors developed Power Management Strategies (PMS) and power grand composite curves technique to adjust RESs integrated SGs operation in response to consumers' load demand. Prosumers based Energy Management and Sharing (PEMS) system is introduced in [34] to evaluate and interpret the role of prosumers in future SGs. The prosumers-centred approach enhances the reliability and sustainability of future SGs. A novel MILP paradigm is introduced in [35] to perform optimal load, renewable energy generation, and resource management scheduling. The purpose is to ensure reliable and sustainable provisioning of energy subjected to maintaining user comfort.

2.2. Stochastic Techniques

Stochastic techniques have emerged in the literature to address the limitations of mathematical methods [36–43]. For example, in [44], non-sorting Genetic Algorithm (GA) based controller is introduced for optimal energy management in smart homes with primary objectives like carbon emissions, energy cost, and peak energy consumption minimization. Likewise, in [45], authors proposed a novel stochastic algorithm to shift load to the battery in peak hours and to the grid in off-peak hours to ensure energy cost minimization. A cascaded technique of GA and MILP is introduced in [46] to solve the economic dispatch problem. Authors in [47] developed an energy management scheme where mutation operator of GA and key steps of ACO are integrated to avoid premature convergence at local optima and obtain the global optimal solution to minimize PAR and energy cost.

Similarly, in [48], authors developed an optimal scheduling scheme for home appliances' power usage pattern management to mitigate PAR and alleviate appliances' waiting time. However, carbon emission and energy cost minimization is ignored. Authors in [49] introduced Firefly Algorithm (FA) to solve the appliances' power usage scheduling problem of smart homes using Critical Peak Pricing (CPP) and Real Time Pricing (RTP) schemes. The objectives are achieved at the cost of compromised user comfort. In [50], the authors introduced Grey Wolf Accretive Satisfaction Algorithm for DSM to ensure the lowest energy cost and highest user comfort. A Candidate Solution Updating Algorithm (CSUA) is introduced in [48]. The purpose is to minimize PAR and appliance waiting time subjected to the desired user comfort level. In [51], authors developed a mechanism that handles uncertainties in consumer behavior and optimally schedules consumers' power usage patterns. In [52], authors developed an online energy management method to cater energy crisis issues in the SG via power usage scheduling. The authors in [53] developed IoT based energy management system for smart communities. The developed model is validated via hardware and software results. In [54], authors developed a hybrid pricing model of RTP signal and Inclined Block Rate (IBR) signal to solve rebound peaks problem via scheduling power usage pattern in smart home for minimizing energy cost and PAR. The authors developed Aquifer Thermal Energy Storage (ATES) approach to minimize energy usage during on-peak hours. The work in [55] proposed cloud and edge computing-based hierarchical framework with distributed architecture to solve energy management problem intelligently. Besides, the developed model also includes real-time communications, collecting information, processing, monitoring, and controlling in households and power grid levels. Results illustrate that the developed model is superior than the other models in aspects of energy management. In [56], authors provide a game-theoretical energy management strategy that schedules the entire electricity consumption of Thermostatically Controlled Load (TCL) consumers. In [57], authors employed heuristic optimization approaches like GA, PSO, and ACO algorithms to schedule power usage patterns in the presence of RESs and ESSs. The authors in [58] proposed an energy management framework with distributed ESSs for users' energy cost and discomfort minimization. The work in [59] developed an optimization-based scheduling framework to adapt power usage patterns of consumers under demand utility and RESs using RTP signal. The purpose is to minimize energy cost, peak energy consumption, and carbon emissions to resolve the rebound peaks problem. The work in [60] introduced a multi-domain communication network with extensible message presence protocol and IEC-61850 framework for meaningful communication between SGs and virtual power plants. In [61], the authors proposed a privacy-preserving model where each node utilizes a dataset for state changes and broadcasts a noisy version. Results show that both the proposed algorithms protect and ensure users' privacy. Nevertheless, end solution optimality and convergence is retained. In [62], authors analyzed the impact of ESSs on the functioning of power systems using a multi-objective cuckoo search algorithm. The Stackelberg game-theoretic framework is introduced in [63] to examine interactions between generators and microgrids for the purpose of maximizing payoffs. The authors in [64] presented a novel technique to fully utilize distributed energy resources using ANN. In [65], authors developed a methodology using Markov Decision Process (MDP) for power usage scheduling in SG for energy expenditure minimization. The authors in [66] conducted a study on reactive and active power flow regulation in islanded distributed microgrids. In [67,68], authors employed an optimum DR to Plugin Hybrid Electric Vehicles (PHEVs) aggregated at parking stations for contributing as ESSs and supplying in the power grid to obtain energy balancing equilibrium.

2.3. Control Techniques

Control techniques emerged as a novel solution to solve problems accompanied by stochastic methods [69–77]. For example, in [78], the authors presented a method for power usage scheduling in SG using Model Predictive Control (MPC). The framework considered RESs, ESSs, and smart loads for optimal distributed DSM. The authors in [79] proposed

a model for energy optimization of solid oxide fuel cell, PV system, nickel-metal-hybrid battery, and load. An integrated Proportional-Integral (PI) and Adaptive Neuro-Fuzzy Inference System (ANFIS) model was used for balancing demand with supply. In [80], authors presented a grid-connected scheduling framework using Distributed MPC (DMPC) to optimize the results. The DMPC results obtained from real-time hardware are same like Centralized MPC (CMPC) results. In contrast, the computational speed of DMPC is faster than CMPC. The work in [81] proposed a hybrid prediction model of ensemble learning network and MPC to forecast interrupted/non-interrupted data for microgrids based energy management. The authors in [82] developed a coordinated MPC model that considers RESs variations and meteorological circumstances while scheduling charging/discharging of batteries and load in microgrids. In [83], dynamic scheduling framework is introduced for grid-connected microgrid operation optimization. Smart metering system and MPC collect energy consumption data of users and pricing signals utility. In this work, which is the continuation of the previous work in [84], a joint scheduling of load (power flexible, time flexible, and base appliances) and energy storage (ESS and EVs) using FPS is exploited for a smart home to achieve objectives such as energy cost, carbon emission, and PAR minimization. A brief comparison of the existing work compared to the proposed model is summarized in Table 1.

The above-discussed techniques from mathematical, stochastic, and control models effectively perform DSM; however, some models are suitable only for specific objectives, constraints, and scenarios. All objectives and scenarios are not considered simultaneously. On this note, this work presents an ACO algorithm based optimal energy management framework to solve DSM problem via power usage scheduling using FPS in smart grid.

Table 1. Summary of related work in aspects of objectives, sources, algorithms, and storage systems, where RESs is Renewable Energy Sources, ESSs is Energy Storage Systems, CG is Commercial Grid, and MGT is Micro Gas Turbine.

Ref.	Generation Sources	Storage Systems	Objectives	Techniques
[7]	RESs+CG	ESSs+MGT	PAR and energy cost	MILP
[8]	RESs+CG	ESSs	Energy cost and complexity	MINLP
[9]	RESs+CG	ESSs	Energy cost and user discomfort	MILP
[10]	RESs+CG	ESSs	Energy cost	ACO, GA, and Knapsack
[30]	RESs+CG	ESSs	Energy cost and PAR	Game theory
[31]	RESs+CG	ESSs	Energy cost	MILP
[32]	RESs+CG	ESSs	Energy cost	MILP
[33]	RESs+CG	ESSs	Energy balancing	PGCC, MILP
[34]	RESs+CG	ESSs	Energy fluctuations	PEMS, MILP
[35]	RESs+CG	ESSs	Bill savings	MILP
[44]	RESs+CG	ESSs	Carbon emission and energy cost	GA
[45]	RESs+CG	ESSs	Energy cost and user comfort	Controllers
[46]	RESs+CG	ESSs	Economic dispatch, PAR and energy cost	GA and MILP
[47]	RESs+CG	ESSs	Premature convergence, PAR and energy cost	ACO
[48]	RESs+CG	ESSs	PAR and delay time	CSUA
[49]	RESs+CG	ESSs	Energy cost	FA
[50]	RESs+CG	ESSs	Energy cost and user discomfort	GWASA
[51]	RESs+CG	ESSs	Optimal scheduling	DR
[52]	RESs+CG	ESSs	Cost, comfort, and delay time	DES
[53]	RESs+CG	ESSs	Energy cost	IoT-based system
[54]	RESs+CG	ESSs	Cost and PAR	ATES
[55]	RESs+CG	ESSs	Energy cost	Hierarchical architecture
[56]	RESs+CG	ESSs	Scheduling	GTDSM
[57]	RESs+CG	ESSs	Energy cost and PAR	GA, PSO, and ACO
[58]	RESs+CG	ESSs	Energy cost and User discomfort	DES
[59]	RESs+CG	ESSs	Energy cost and PAR	HGACO

Table 1. *Cont.*

Ref.	Generation Sources	Storage Systems	Objectives	Techniques
[60]	RESs+CG	ESSs	VPP management	XMPP based IEC 61850 communication
[61]	RESs+CG	ESSs	Charging/Discharging scheduling	Privacy-preserving
[62]	RESs+CG	ESSs	DSM	CSA
[63]	RESs+CG	ESSs	Maximizing payoffs	Stackelberg game theory
[64]	RESs+CG	ESSs	Energy resources optimization	ANN
[65]	RESs+CG	ESSs	Energy cost	MDP
[66]	RESs+CG	ESSs	Reactive power flow control	PCC
[67]	RESs+CG	ESSs	Energy balancing a	Stochastic optimization
[78]	RESs+CG	ESSs	Energy cost	MPC
[79]	RESs+CG	ESSs	Energy cost	PI and ANFIS
[80]	RESs+CG	ESSs	Energy cost	DMPC
[81]	RESs+CG	ESSs	Energy cost	MPC
[82]	RESs+CG	ESSs	Green house gases	MPC
[83]	RESs+CG	ESSs	Energy savings	MPC

3. Proposed Optimal Demand-Side Management Framework

The proposed optimal DSM framework comprises an energy management system (EMS), microgrid, and graphical user interface (GUI). The EMS consists of energy management center (EMC), advanced metering infrastructure (AMI), home appliances, and home gateway (HG). The AMI of EMS acts as a central nervous system enabling two-way communication between the utility and consumers to collect and transmit power usage data to utility and send demand response (DR) signal from utility to EMC in real-time. The EMC is embedded in HG that receives DR signal via HG to create power usage schedule as per the priority and constraints of users and utility. The home is considered to have three types of smart appliances: time flexible appliances like dishwasher, cloth dryer, and EVs; power flexible appliances like AC, heater, and refrigerator; and critical/base appliances. These smart appliances interact directly with EMC via wireless communication links like Z-wave, ZigBee, and Wifi. However, there is a limitation that smart appliances do not interact with each other. The EMC schedule operation of all appliances is based on DR signal, consumers, and utility constraints. The microgrid part of the developed framework consists of WT, PV panels, EVs, batteries, and MGT. The microgrid generation is stochastic in nature due to its dependence on changing weather conditions. Thus, ANN-EDE model is developed for prediction and estimation of microgrid generation profile. The GUI part either has IDD or remote devices like mobile or laptop, which is used to monitor and control the whole process of EMS power usage scheduling. The developed DSM framework is shown in Figure 1. The detailed description of the developed framework is as follows:
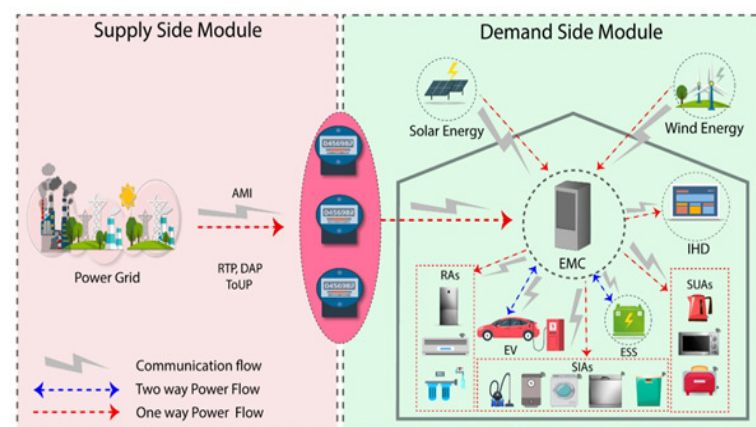

Figure 1. Developed framework for optimal DSM in SG.

3.1. Prediction Model for Microgrid Generation Estimation

This section presents ANN-EDE prediction model that estimates microgrid generation by forecasting solar irradiance and wind speed, as shown in Figure 2. Similarly, some hybrid models are used for load prediction in literature [85,86]. The developed prediction framework has forecasting and optimization modules. The forecaster module uses ANN for prediction of wind speed and solar irradiance for accurate microgrid energy generation estimation based on history data received as input. The ANN layers like input, hidden, and output having artificial neurons are activated via sigmoidal activation function [84] to generate output. These layers are connected in feed-forward fashion, where the preceding layer gets input from earlier layers. The sigmoidal activation function is defined as follows in Equation (1) [84]:

$$f(S,b) = \frac{1}{1 + e^{-\beta(S-b)}} \tag{1}$$

where S represents input signal with selected attributes, parameter β determines the steepness of sigmoidal function, and b shows bias value. The ANN forecaster employed multivariate autoregressive rule to learn from history data to predict wind speed and solar irradiance for accurate energy estimation [84]. The prediction model is shown as first block in Figure 2. The history data is adopted from [84]. The history data is divided into training and testing sets of 80% and 20%, respectively. The training set trains the model to forecast solar irradinace and wind speed, and the testing set validates the model by comparing obtained results with ground truth observations. The MAPE error is employed as a performance metric mathematically defined as follows in Equation (2) [84]:

$$MAPE(i) = \frac{1}{n} \sum_{j=1}^{m} \frac{\left| p^a(i,j) - p^f(i,j) \right|}{p^a(i,j)} \tag{2}$$

where $p^a(i,j)$ represents real and $p^f(i,j)$ shows predicted solar irradiation and wind speed. m is the number of days. Levenburg Marquart algorithm tunes control parameters until the error reaches the lowest value. The predicted solar irradiation and wind speed ANN is given as input to EDE based optimizer for further error minimization. In the optimization module, the error is further minimized using the EDE algorithm depicted in Figure 2. The EDE algorithm is selected due to the following merits: computational efficiency, fast convergence rate, and resolving premature convergence issues. The EDE algorithm optimizes control parameters of ANN for accurate wind speed and solar irradiance prediction to estimate microgrid energy generation.

3.2. Smart Home Appliances

The smart appliances A are classified as time flexible A_a^T, power-adjustable A_a^P, and base A_a^C. $S_t^a = \{1, 0\}$, and $X_t^a = (r_t^a, w_t^a)$ are defined as appliance status, and position indicators, respectively, where r_t^a and w_t^a represents the appliance's remaining hours, and waiting hours, respectively. Complete set of smart appliances is defined as follows:

$$A = \left\{ A_a^T, A_a^P, A_a^C \right\} \tag{3}$$

where A shows a set of smart appliances having three types of appliances. Detailed discussion on each class is as follows:

1. Power adjustable appliances are also known as power regulating appliances having flexible power regulation between maximum and minimum power to participate in the DR program to achieve desired objectives. During peak hours, such appliances operate with maximum power and work with minimum power during off-peak hours

to minimize energy cost, PAR, and carbon emission. The current status and status at the next hour are defined as:

$$X_t^N = (T_P^o, \beta - \alpha + T_P^o + 1) \tag{4}$$

$$X_{t+1}^P = \begin{cases} r_t^P, \ 0, \ P_r^{\min p} & \text{if} S_t = 1, r_t^P \geq 1 \\ r_t^P, \ 0, \ P_r^{\max p} & \text{if} S_t = 1, r_t^P \geq 1 \\ 0, \ 0 & \text{otherwise} \end{cases} \tag{5}$$

where X_t^P and X_{t+1}^P denote current status and status at the next hour, respectively. T_P^o represents the length of operation hours, α represents operation starting hour, and β represents operation ending hour. $P_r^{\min p}$ and $P_r^{\max p}$ represent minimum and maximum power, respectively.

2. Time adjustable appliances have flexible operating time and fixed rated power. Time flexible appliances are classified into two types: non-interruptible A_T^{NI} and interruptible A_T^I, which are defined as follows:

$$A_a^T = \left\{ A_T^I, A_T^{NI} \right\} \tag{6}$$

- Interruptible appliances A_T^I are also known as deferrable appliances that can tolerate interruption, advance, and delay in operation even during running time. The current status and status at the next hour are modeled as follows:

$$X_t^I = (T_I^o, \beta - \alpha + T_I^o + 1) \tag{7}$$

$$X_{t+1}^I = \begin{cases} r_t^I, \ w_t^I - 1, \ P_r^I & \text{if} S_t = 0, w_t^I \geq 1 \\ r_t^I - 1, \ w_t^I \ P_r^I & \text{if} S_t = 1, r_t^I \geq 1 \end{cases} \tag{8}$$

where X_t^I and X_{t+1}^I represent current status and status at the next hour, respectively, T_I^o shows the length of operation hours.

- Non-interruptible appliances A_T^{NI} can tolerate delay/advance before the operation starts and cannot tolerate interruption during work. Current status and status at the next hour are defined as:

$$X_t^N = (T_N^o, \beta - \alpha + T_N^o + 1) \tag{9}$$

$$X_{t+1}^N = \begin{cases} r_t^N, \ w_t^N - 1, \ P_r^{NI} & \text{if} S_t = 0, w_t^N \geq 1 \\ r_t^N - 1, \ 0, \ P_r^{NI} & \text{if} S_t = 1, r_t^N \geq 1 \end{cases} \tag{10}$$

where X_t^N and X_{t+1}^N shows current status and status at the next hour, respectively, T_N^o shows the length of operation hours.

3. Critical appliances work on fixed power without interruption and cannot tolerate delay or advance in operation.

Constraints and parameters of smart appliances are presented in Table 2.
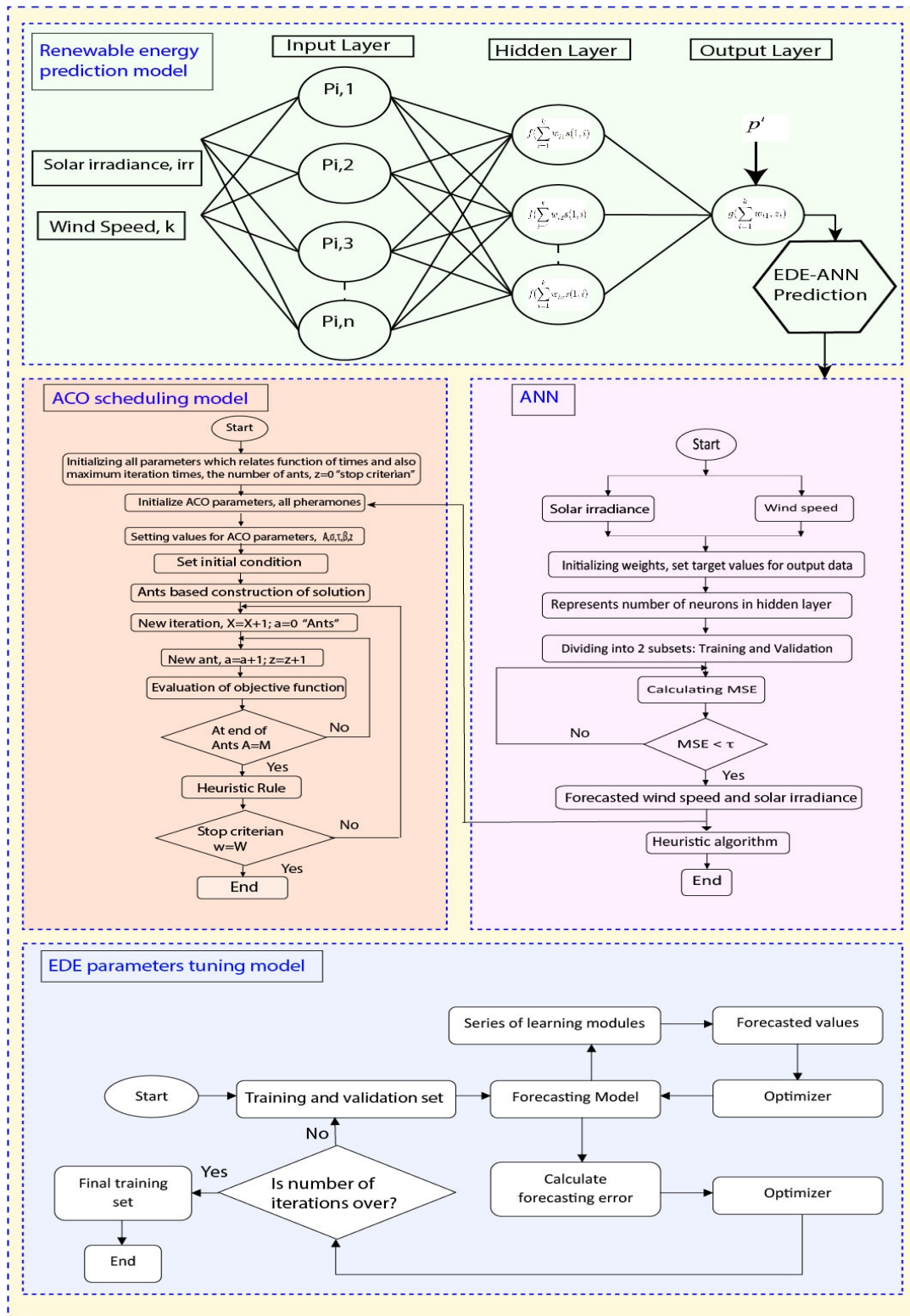
Figure 2. Developed optimal DSM framework working flow chart.

Table 2. Smart appliances control parameters like duration, operation time interval, priority, etc.

Type	Device	Time (hours)	Rated Power (kW)	Start Time	End Time	Priority
Time flexible appliances						4
Interruptible time flexible appliances	Washing machine	6	3.0	9:00 am	3:00 pm	
	Tumble dryer	4	3.3	4:00 pm	8:00 pm	
	Dishwasher	2	2.5	10:00 pm	12:00 am	
Non-interruptible time flexible appliances						3
	Vacuum cleaner	2	1.5	10:00 am	12:00 pm	
	Water heater	3	1.8	5:00 am	8:00 am	
Power flexible appliances						2
	Refrigerator	24	0.5–1.5	8:00 am	8:00 am	
	Airconditioner	24	0.8–1.8	8:00 am	8:00 am	
	Water dispenser	24	0.5–2.0	8:00 am	8:00 am	
Base appliances						1
	Microwave oven	2	1.2	2:00 pm	4:00 pm	
		2	1.9	8:00 am	1:00 am	
	Electric kettle	2	1.9	4:00 pm	6:00 pm	
		2	1.9	8:00 pm	10:00 pm	
		2	1.2	7:00 am	9:00 am	
	Electric toaster	2	1.2	1:00 pm	3:00 pm	
		2	1.2	8:00 pm	10:00 pm	

3.3. Microgrid

A microgrid has solar PV and WT for electricity generation. Microgrid's net electricity generation is mathematically modeled in Equation (11).

$$E(t) = \sum_{m\varepsilon M} \varepsilon m(t) \tag{11}$$

where εm shows single RES electricity generation, the net energy generation of microgrid during 24 h is as modeled as follows:

$$E(t) = \sum_{t=1}^{T} \sum_{m\varepsilon M} \varepsilon m(t) \tag{12}$$

3.3.1. Wind Energy Generation System

WT generates energy at output based on wind speed, which is defined in Equation (13) as follows:

$$P^{wt}(t) = 1/2 \times C_p \times (\lambda) \times \rho \times A \times (V_t^{wt})^3 \tag{13}$$

where P^{wt}, A, V_t^{wt}, and ρ, represent WT energy, turbine blades area, wind speed, and air density, respectively. The relation between electricity generation and wind speed is depicted in Figure 3. The ANN-EDE forecasts wind speed for accurate energy estimation [87], which is shown in Figure 2. The wind energy system speed constraints are modeled in Equations (14)–(16).
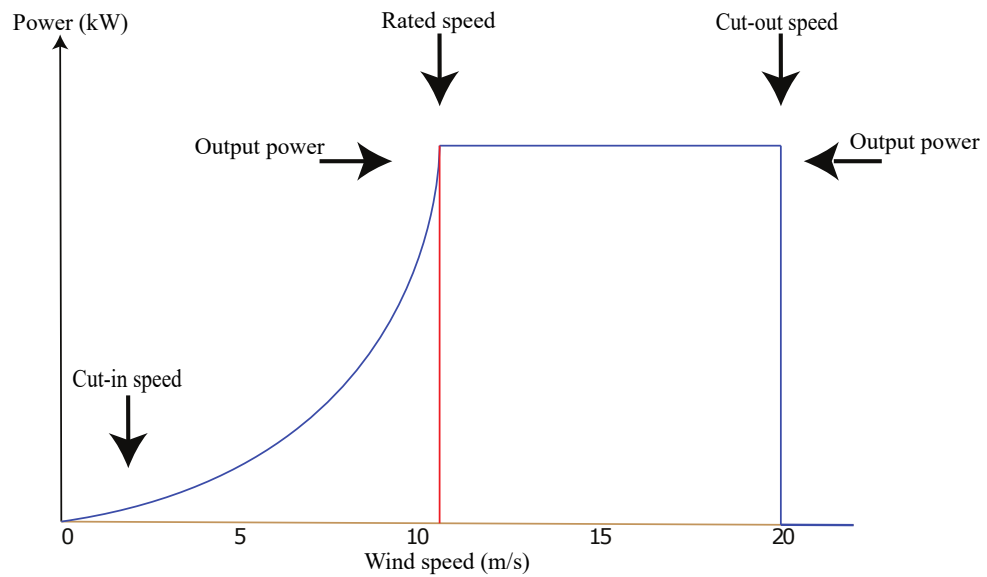
Figure 3. WT electricity generation with rated, cut-in, and cut-out speed.

$$V^{cut-in} \leq V^{wt}(t) \leq V^{cut-out} \tag{14}$$

$$0 = V^{wt}(t) \geq V^{cut-out}, \forall t \varepsilon T \tag{15}$$

$$0 = V^{wt}(t) \leq V^{cut-in}, \forall t \varepsilon T \tag{16}$$

3.3.2. Solar PV Energy Generation System

The ANN-EDE model forecasts solar irradiance for accurate energy estimation [87], which is shown in Figure 2. Solar PV system generates electricity from the sun depending upon forecasted solar irradiation, and ambient temperature, defined as follows [88]:

$$P_t{}^{pv} = \eta^{pv} \times A^{pv} \times Irr(t) \times (1 - 0.005(Temp(t) - 25)) \tag{17}$$

where $P_t{}^{pv}$ is electrical energy generation, A^{pv} is area of solar panel, η^{pv} is efficiency of solar panel, $Irr(t)$ is solar irradiance, and $Temp(t)$ is ambient temperature. The i-v curve with Maximum Power Point Tracking (MPPT) is shown in Figure 4 that assures PV cell optimal performance.
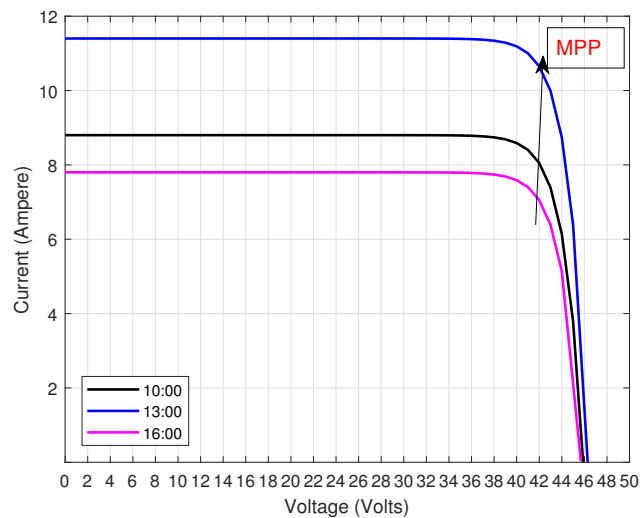
Figure 4. Solar cell I-V curve.

4. Energy Management Problem Formulations

The energy management problem stated in this work is formulated as a minimization problem with objective functions like carbon emission, energy cost, and PAR. The complete modeling and formulation is as follows:

4.1. Objective Function

The objective function of the proposed model is based on energy cost, PAR, and carbon emission, which is modeled as a minimization problem depicted in Equation (18).

$$\text{mini} \sum_{t=1}^{T} \begin{pmatrix} (E^t + ESS^t + EV^t + MGT^t) \\ \times (EP_t + \mu_t + Y_t) \end{pmatrix} \tag{18}$$

This work aims to schedule appliances and EVs/batteries charging/discharging for energy cost EP_t, PAR μ_t, and carbon emission Y_t minimization subjected to the following constraints (19)–(43).

$$E(t) = P^{pv}(t) + P^{wt}(t), \tag{19}$$

$$A_a^T + A_a^T + A_a^C = \begin{pmatrix} E(t) + ESS(t) + EVs(t) \\ + MGT(t) + \Phi(t) \end{pmatrix} \tag{20}$$

$$\sum_{a=1}^{n} \eta = LOT(a), \tag{21}$$

$$\sum_{a=1}^{n} \alpha \leq \eta \leq \beta, \tag{22}$$

$$\Phi_t \leq KI, \tag{23}$$

$$V^{cut-in} \leq V(t)^{wt} \leq V^{cut-out}, \qquad \forall t \, \varepsilon \, T, \tag{24}$$

$$0 < Irr(t) < kc, \qquad \forall t \, \varepsilon \, T, \tag{25}$$

$$0 < ESS_{\min} < ESS_{\max}, \qquad \forall t \, \varepsilon \, T, \tag{26}$$

$$EVs_{\min}^e \leq \rho EVs_a^e + EV_e \leq EVs_{\max}^e \tag{27}$$

where Equation (19) shows the overall contribution of microgrid generation to the overall electricity generation. PV contributes 20%, WT contributes 30%, and utility contributes 50%. Equation (20) ensures that appliances are optimally scheduled, and Equation (21) represents the total operation time slots of appliances. Constraint (22) represents ON/OFF appliances status. Equation (23) represents hourly imported energy. Equation (24) shows hourly wind energy generation with cut-in and cut-out speeds. Equation (25) shows solar irradiance. The Equation (26) shows charging levels like maximum and minimum. Equation (43) shows energy consumption of EVs considering arrival and departure time.

4.1.1. Energy Cost

Energy cost using FPS per hour W/O considering microgrid is modeled as follows:

$$\zeta(t) = (\Gamma_{A_a^T}(t) + \Gamma_{A_a^P}(t) + \Gamma_{A_a^C}(t)) \times EP(t) \tag{28}$$

where $\Gamma_{A_a^T}(t)$, $\Gamma_{A_a^P}(t)$, and $\Gamma_{A_a^C}(t)$ are per hour energy consumption of time flexible appliances, power flexible appliances, and critical/base appliances, respectively. The net energy cost per day is shown by Equation (29).

$$\zeta(T) = \sum_{t=1}^{T} (\Gamma_{A_a^T}(t) + \Gamma_{A_a^P}(t) + \Gamma_{A_a^C}(t)) \times EP(t) \tag{29}$$

The imported energy considering microgrid including ESSs, EVs, and MGT is expressed in Equation (30).

$$\Phi(t) = \left(\begin{array}{l} (\Gamma_{A_a^T}(t) + \Gamma_{A_a^P}(t) + \Gamma_{A_a^C}(t)) - (E(t)+ \\ EVs.\alpha_{EVs(t)} + ESS.\alpha_{ESS(t)} + MGT.\alpha_{MGT(t)}) \end{array} \right) \tag{30}$$

$$\Phi(t) = \begin{cases} \Phi(t) & if\ \Phi(t) > 0, \\ 0 & otherwise \end{cases} \tag{31}$$

Per hour and per day energy cost is defined in Equations (32) and (33), respectively.

$$\delta(t) = (\Phi(t) \times EP(t)) \tag{32}$$

$$\delta(t) = \sum_{t=1}^{T} (\Phi(t) \times EP(t)) \tag{33}$$

4.1.2. PAR

PAR minimization is one of our objectives, which is beneficial for utility grid and consumers because it leads toward cost minimization for both bodies. PAR minimization objective is catered W/O and with microgrid, which is mathematically modeled as follows:

$$L_{avg} = \frac{1}{T} \sum_{t\varepsilon T} L_t \tag{34}$$

$$L_{\max} = \sum_{t\varepsilon T} \max L_t \tag{35}$$

$$\mu = \frac{L_{\max}}{L_{avg}} \tag{36}$$

where Equations (34)–(36) represent average energy consumption, peak energy consumption, and PAR, respectively.

4.1.3. Carbon Emission

Carbon emission minimization is one of our objectives that highly contribute to a sustainable, neat, and clean environment. Existing literature used diesel generators as backup, which release more carbon emission and cause global warming. Thus, we employed MGT with RESs in a microgrid instead of a diesel generator as a backup to ensure carbon emission minimization to participate in a clean and green environment. Carbon emission is mathematically modeled as follows:

$$Y = \frac{avg\ EP}{\varepsilon \times \varsigma \times \Im} \tag{37}$$

where in Equation (37) symbols like $avg\ EP$, ε, ς, and $\Im$, average energy price, energy price per kWh, emission factor, and hours, respectively.

4.2. MGT

MGT is utilized as a shiftable energy generation source with generation capacities from 15–300 kW. MGT produces low cost energy than diesel generator because diesel is more expensive than natural gas. The MGTs have significant impact on carbon emission reduction. It is imperative to remember that MGT has two binary states: ON and OFF; it generates 2 kW power when switched on and otherwise generates 0 kW.

4.3. Energy Storage Devices

This work considers two types of energy storage devices: batteries (ESSs) and EVs. Both types are discussed in detail as follows:

4.3.1. ESSs

ESSs are batteries that convert various energy sources to electrical energy and deliver electrical power whenever required. The smart home has ESSs with storage capacity of 3 kWh as catered in [89], and has minimum and maximum charging/discharging levels defined in [88]. Complete modeling is defined as follows:

$$SE(t) = SE(t-1) + k.\eta^{ESSs}.ES^{ch}(t) - k.ES^{dis}(t)/\eta^{ESSs} \tag{38}$$

$$ES(t)^{ch} \leq ES_{\max} \tag{39}$$

$$ES(t)^{dis} \geq ES_{\min} \tag{40}$$

$$ESSs(t)^{ch} < ESS_{upl} \tag{41}$$

$$\alpha_e(t) = \begin{cases} 1 & if \ ESSs \ is \ ch\arg ing, \\ -1 & if \ ESSs \ is \ disch\arg ing, \\ 0 & if \ ESSs \ is \ idle. \end{cases} \tag{42}$$

where SE denotes stored energy (Ah) at time duration t, η^{ESSs} represents ESSs energy efficiency, $ES^{ch}(t)$ and $ES^{dis}(t)$ represents charging/discharging status per hour modeled in Equation (42).

4.3.2. EVs

This work employs EVs as a storage device to increase savings and minimize energy costs. EVs can be used for both storage and driving, which is modeled in Equation (43).

$$EV_e = \sum_{t=t_d^e}^{t_d^e} (\psi_e(t) \times \alpha_e(t)) \tag{43}$$

The developed model is implemented in MATLAB, and obtained results are discussed in the subsequent section.

5. Performance Evaluation: Results and Discussions

The developed model is implemented in MATLAB 2018b installed on Intel Core i5 laptop with 8 GB of RAM and 2.4 GHz processor. Results obtained from experiments of the proposed and existing models are evaluated in aspects of objectives like energy cost, carbon emission, PAR, and user discomfort minimization for two scenarios: energy management via scheduling W/O considering microgrid, and energy management via scheduling with microgrid. Furthermore, smart appliances are divided into three groups, and complete description of appliances are depicted in Table 2. The ACO based EMC creates operation schedule of appliances for day-ahead time horizon using FPS, shown in Figure 5, which reduces energy cost, PAR, and carbon emission. The detailed description of each scenario is given as follows:
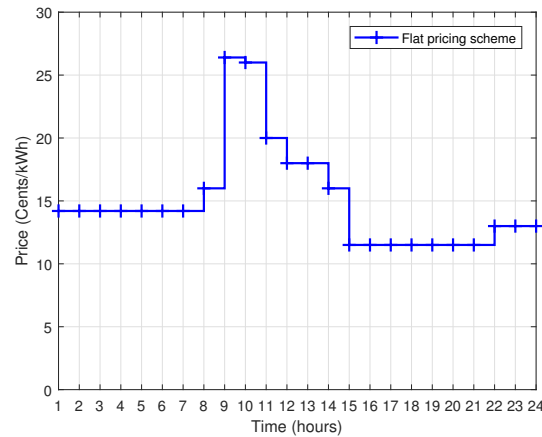
Figure 5. Utility advertised flat pricing scheme.

5.1. Scenario I: Energy Management via Scheduling W/O Considering Microgrid

This section discusses the simulation results of developed ACO compared to existing models for power usage scheduling W/O considering the microgrid. Figure 6 shows that the developed algorithm schedules the load during low price hours as per the FPS W/O considering the microgrid. Figure 6 illustrates that energy consumption is maximum without implementing our developed model because energy is purchased and used during high price hours that lead to peaks creation in demand. Numerical results are listed in Table 3.

Table 3. Overall evaluation of the developed ACO algorithm compared to MILP and W/O scheduling case in aspects of carbon emission, energy cost, and PAR.

Scenarios	Models	Carbon Emission (%)	Energy Cost (%)	PAR (%)
Scenario-I: W/O microgrid				
	MILP	7.28	15.66	17.2
	ACO	15.35	23.69	26.20
Scenario-I: With microgrid				
	MILP	10.20	17.13	11.29
	ACO	18.5	25.09	31.45
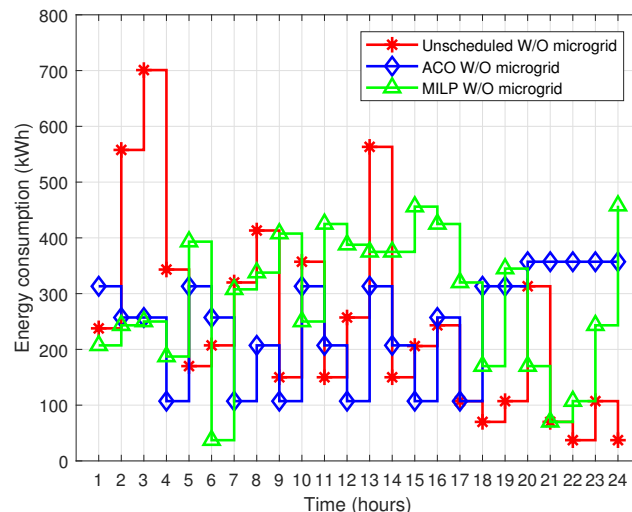
Figure 6. Energy consumption evaluation W/O considering microgrid.

The per hour energy cost profile of the discussed energy consumption is shown in Figure 7. Figure 7 demonstrates that consumers pay the least bill with our proposed model than unscheduled and MILP based scheduling cases. Our developed model optimally schedules appliances during off-peak hours, and eventually, consumers pay the minimum cost and enjoy savings in the utility bill.
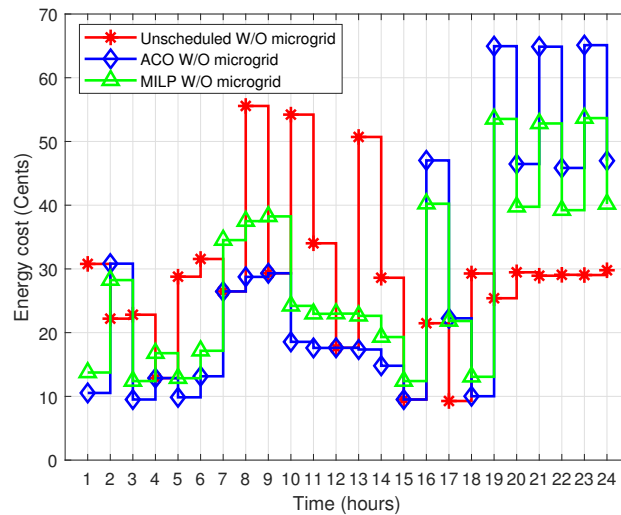
Figure 7. Energy cost evaluation W/O considering microgrid.

Figure 8 illustrates per day energy cost evaluation of the developed model compared to MILP and W/O scheduling case. It is obvious from the figure that our model reduced a significant cost compared to unscheduled and MILP based cost. Thus, the developed model outperforms existing models in aspects of energy cost minimization, and achieved cost reduction of 23.69%. Numerical results are listed in Table 3.
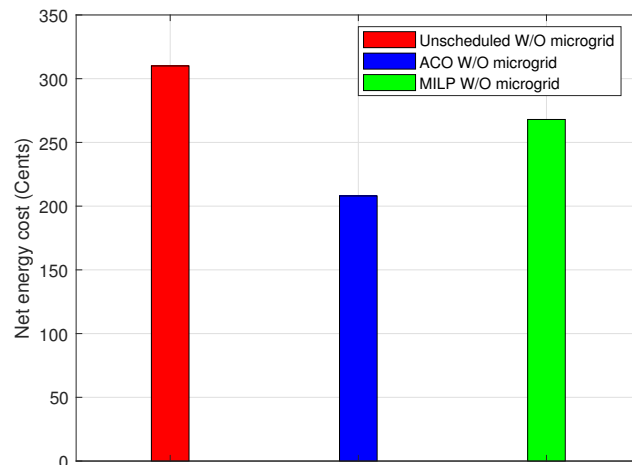
Figure 8. Energy cost per day evaluation.

Figure 9 shows PAR minimization evaluation of the developed ACO, MILP, and W/O scheduling case. It is evident that the developed ACO algorithm has the lowest PAR compared to MILP and W/O scheduling case. The reduction achieved is 26.20%. Numerical results are listed in Table 3.
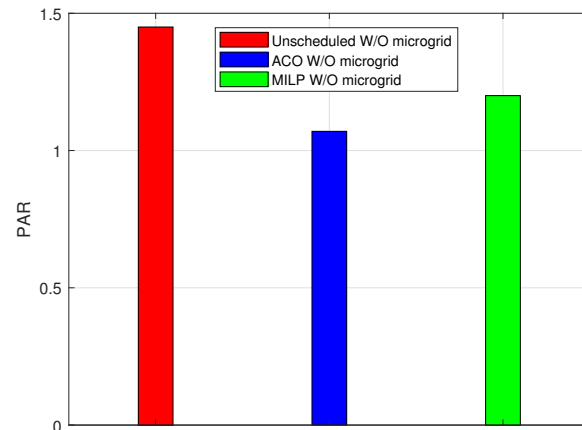
Figure 9. PAR minimization evaluation W/O considering microgrid.

The comparative analysis of carbon emission minimization (ACO, MILP, and unscheduled) is depicted in Figure 10. The developed ACO algorithm emits less carbon than MILP and W/O scheduling case. The maximum carbon emission recorded during hours 19–23 is 149 pounds for the W/O scheduling case. In contrast, the MILP model emits maximum carbon of 147 pounds during the same hours. The developed ACO algorithm emits maximum carbon of 140 pounds during the same hours, which is minimum per hour carbon emission than MILP and W/O scheduling case. Numerical results are listed in Table 3. Thus, the ACO algorithm outperforms MILP and W/O scheduling case in carbon emission minimization.
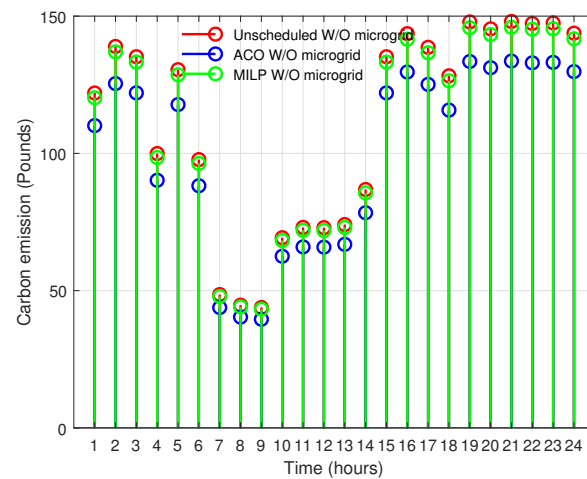
Figure 10. Comparative evaluation of carbon emission minimization.

5.2. Scenario II: Energy Management via Scheduling Considering Microgrid

Extensive simulations are conducted considering microgrids to solve energy management problem via scheduling based on developed ACO and MILP. The microgrid includes RESs (PV and WT) with ESSs and EVs. The microgrid employs the ANN-EDE model to estimate electricity generation by accurately forecasting wind speed and solar irradiance, which is illustrated in Figure 11. Thus, ANN-EDE based prediction is accurate, having low MAPE and closely following the target observation of wind speed and solar irradiance, leading towards accurate microgrid energy generation estimation. The ANN-EDE results in terms of MAPE error are listed in Table 4. This estimated electricity generation is utilized in the developed framework for energy management.

**Table 4.** Evaluation results of ANN-EDE and ANN prediction models in aspects of MAPE.

Forecasting Profile	Models	MAPE
Solar irradiance	ANN-EDE	0.4942
	ANN	2.6540
Wind speed	ANN-EDE	0.5082
	ANN	2.5350

Microgrid energy generation (PV and WT) is shown in Figure 12. Energy generation from PV energy system during daytime is high because solar irradiation is high and low at night due to lower solar irradiation. For more in-depth understanding, interested readers are referred to read [88]. The energy generation from WT depends on wind speed; when wind speed is high within the cut-out threshold speed, the generation from wind energy is maximum. A detailed discussion on this topic is available in [87].

Charging/discharging behavior of EVs with microgrid is depicted in Figure 13. It is clear that EVs are charging during the time horizon when microgrid generation is high and discharging during the time horizon when microgrid generation is low. In the first hour, EVs have complete charging, and during 11–15 h, EVs have medium charging. During these hours, EVs can serve the load.
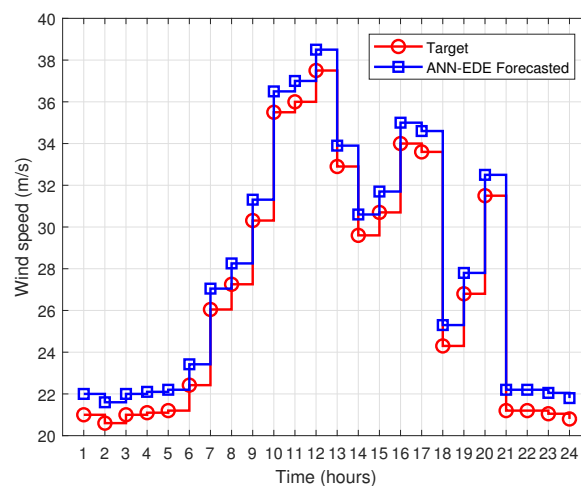
(**a**)
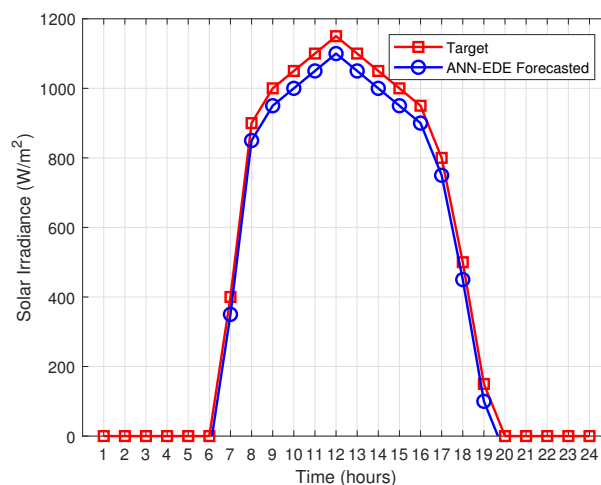
(**b**)

Figure 11. Wind speed and solar irradiance prediction using developed ANN-EDE model for microgrid energy generation estimation. (**a**) Wind speed forecasting. (**b**) Solar irradiance forecasting.
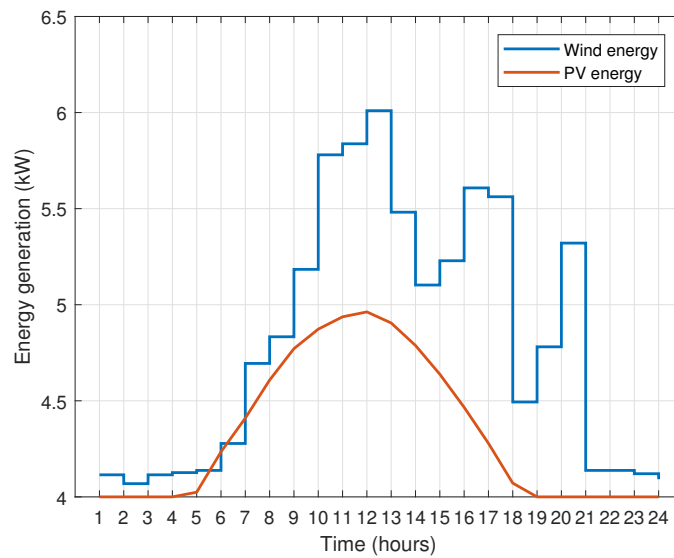
Figure 12. Microgird including PV and WT energy generation.
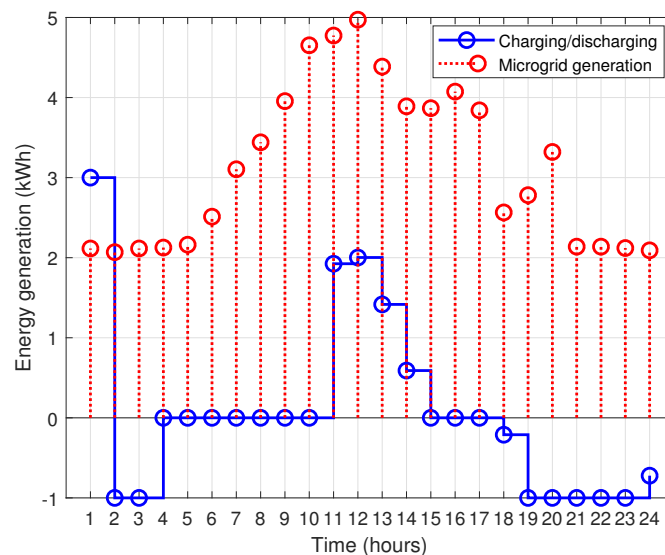

Figure 13. Charging/discharging behavior of EVs with microgrid generation.

The contribution of EVs and ESSs in serving the load is depicted in Figure 14. The portion of the load that is served (operated) with EVs and ESSs results in low carbon emission, energy cost, and PAR compared to the portion which utility companies serve. Thus, when EVs and ESSs have significant charging, then there is no need for the consumers to import electricity in the following conditions: during peak hours, and when renewable generation is minimum. EVs and ESSs will serve the load to reduce carbon emission, energy cost, and PAR during such a situation.
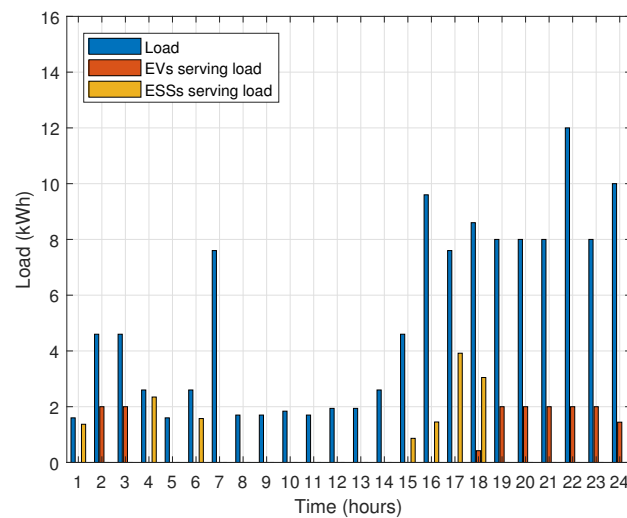
Figure 14. Contribution of EVs and ESSs in serving load.

Net energy demand and imported/purchased energy from the utility with and W/O EVs discharging abilities are depicted in Figure 15. It is evident from the results that the developed model significantly reduced the import of energy in peak hours. Furthermore, consumers import minimum energy when utilizing EVs for discharging. On the other side, consumers import more energy when EVs are not fully charged and cannot discharge.
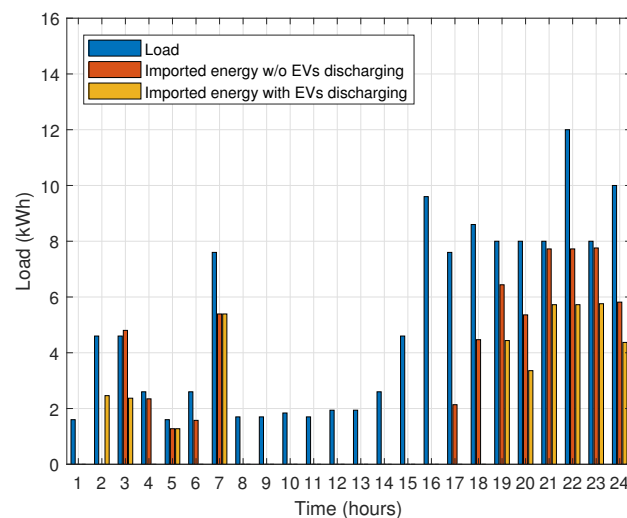

Figure 15. Imported/purchased energy with and W/O EVs discharging.

The diesel generator, when used with microgrid as a backup, releases a lot of carbon into the environment, which highly contributes to pollution. Thus, adopting a diesel generator as a back source is not a vital solution. On this note, MGT with microgrid is used as a backup source, which highly contributes to reducing carbon emission, leading to a clean environment. The obtained results of carbon emission reduction when MGT is used as backup sources with microgrid are shown in Figure 16. Thus, the use of MGT results in reduction of 25% carbon compared to a diesel generator.
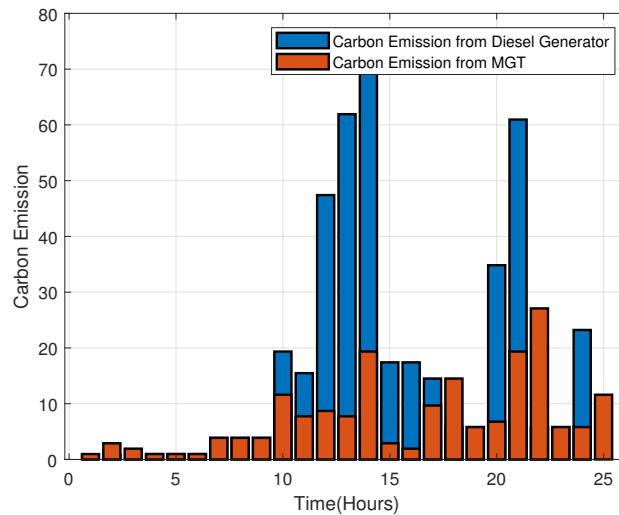
Figure 16. Carbon emission reduction using MGT/diesel generator with microgrid as a backup source.

The users' energy consumption considering microgrid is shown in Figure 17. It is evident from the figure that in W/O scheduling case, the consumers operate mainly appliances in peak hours, which creates high peaks in the demand curve at 1 and 21 h. Similarly, when users schedule appliances with MILP, peaks in energy consumption are significantly reduced compared to the W/O scheduling case. However, ACO algorithm based energy consumption has no peaks compared to MILP and W/O scheduling case. Thus, the developed ACO algorithm based schedule has a smooth demand curve compared to MILP and W/O scheduling case.
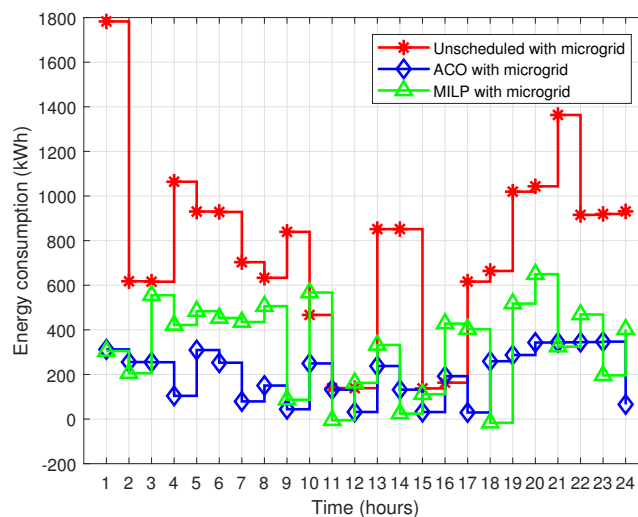
Figure 17. Users' energy consumption considering microgrid.

Energy cost evaluation considering microgrid using ACO, MILP, and W/O scheduling case is depicted in Figure 18. In the W/O scheduling case, the maximum energy cost is 85 cents at hour 1, MILP has 49.5 cents at hour 1, and the developed ACO algorithm is 41.5 cents at hour 2. Thus per hour energy cost of W/O scheduling case for 24 h time horizon is high compared to MILP and ACO. Thus, developed ACO outperforms MILP and W/O scheduling case in aspects of per hour energy cost minimization. Likewise, net energy cost minimization evaluation is illustrated in Figure 19. The net energy cost W/O scheduling for 24 h is 251 cents compared to MILP and developed ACO algorithm, which is 208, and 188 cents, respectively. The energy cost minimization results prove that the ACO

algorithm is more promising than MILP and W/O scheduling case. Thus, the developed ACO based algorithm is more effective in energy cost minimization (both per hour and net) than MILP and W/O scheduling case.
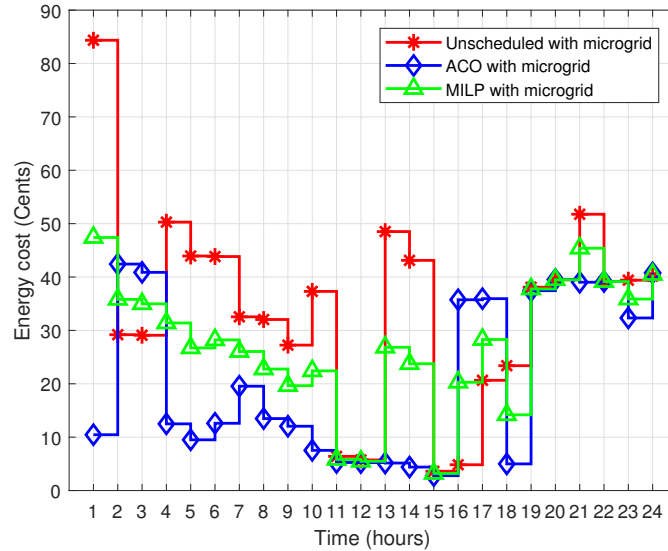

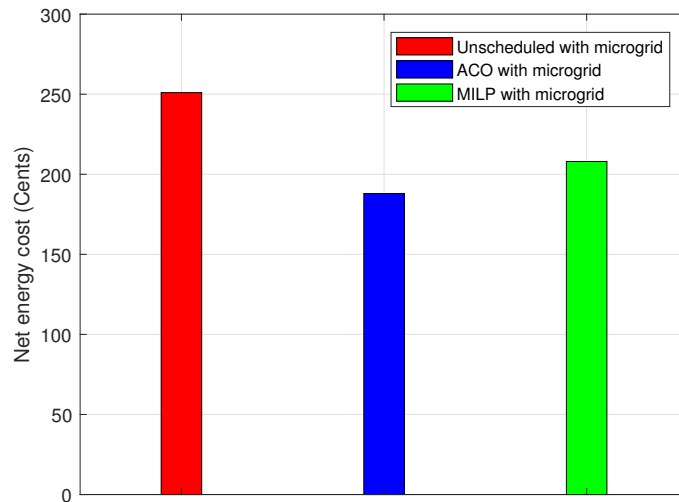**Figure 18.** Per hour energy cost minimization evaluation considering microgrid.

Figure 19. Net Energy cost minimization evaluation considering microgrid.

The PAR minimization evaluation with microgrid based on MILP, ACO, and W/O scheduling case, is shown in Figure 20. The developed ACO algorithm has maximum PAR reduction compared to MILP and W/O scheduling case. The MILP and developed ACO algorithm reduced PAR by 12.5% and 25%, compared to W/O scheduling case, respectively. The ACO algorithm optimally scheduled appliances in low price hours and thus achieved maximum PAR reduction. This PAR reduction is beneficial for both consumers and utility.
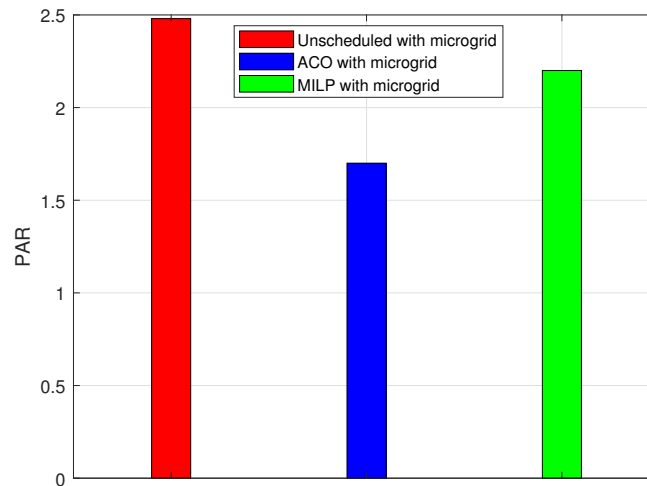
Figure 20. PAR minimization evaluation considering microgrid.

Carbon emission minimization evaluation considering microgrid is depicted in Figure 21. The developed ACO algorithm and MILP result in low carbon emissions than the W/O scheduling case. Carbon emission considering microgrid W/O scheduling is 140 pounds during hours 19-23, which is maximum compared to MILP and developed ACO algorithm. On the other hand, carbon emission considering microgrid with MILP is 121 pounds, which is moderate carbon emission compared to ACO and W/O scheduling case. Likewise, the developed ACO algorithm has 102 pounds during hours 19–23, the which is less than MLIP and W/O scheduling case. Similarly, behavior is observed for the rest of the hours. The developed ACO and MILP reduced carbon emission by 18.5% and 10.20%, respectively, compared to W/O scheduling case. Results illustrate that the developed ACO algorithm has significantly reduced carbon emissions than MILP and W/O scheduling case.
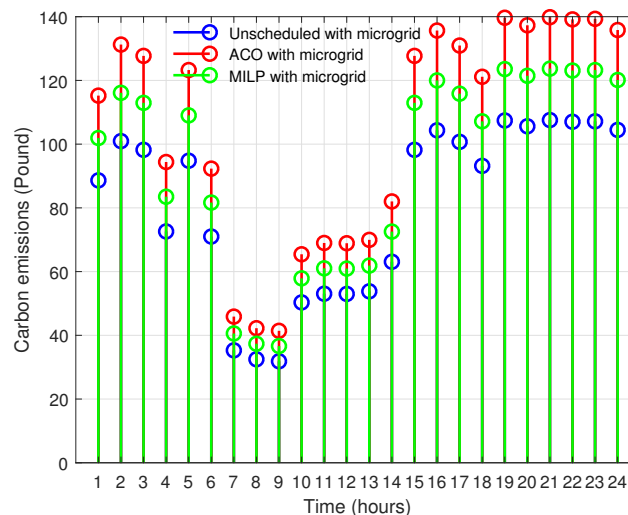

Figure 21. Carbon emission minimization evaluation considering microgird.

Overall evaluation results of the developed ACO algorithm compared to MILP and W/O scheduling case in aspects of carbon emission, energy cost, and PAR minimization are listed in Table 3. Thus, the above results and discussion conclude that the developed model outperforms existing MILP model and W/O scheduling case in terms of carbon

emission, PAR, and energy cost minimization for the two scenarios of with and W/O considering microgrid.

6. Conclusions

This paper proposed and developed a framework to solve the DSM problem with and W/O grid-connected SG. For the proposed framework, we developed ACO algorithm to schedule appliances and charging/discharging behavior of EVs/batteries using FPS. The ANN-EDE prediction model is developed to forecast solar irradiance and wind speed for accurate microgrid energy generation estimation to solve DSM problem optimally. The developed framework aims to minimize PAR, energy cost, and carbon emissions by balancing demand and generation. The proposed framework is evaluated by comparing it with MILP and W/O scheduling case. The ACO algorithm reduced energy cost, PAR, and carbon emission by 23.69%, 26.20%, and 15.35% in scenario I, and 25.09%, 31.45%, and 18.50% in scenario II, respectively, as compared to W/O scheduling case. Results show that the developed ACO algorithm outperformed MILP and W/O scheduling case in aspects of the desired objectives and is beneficial for both utility and consumers.

References

1. Energy Reports. Available online: http://www.enerdata.net/enerdatauk/press-and-publication/energyfeatures/infuture-2007.php (accessed on 10 February 2021).
2. FERC. Demand Response Compensation in Organized Wholesale Energymarkets, FERC Docket RM101700. Available online: http://www.ferc.gov/eventcalender/files/20110315105757RM101700.pdf (accessed on 18 March 2021).
3. Kamran, M. Current status and future success of renewable energy in Pakistan. *Renew. Sustain. Energy Rev.* **2018**, *82*, 609–617. [CrossRef]
4. Ghulam, H.; Khan, I.; Jan, S.; Shah, I.A.; Khan, F.A.; Derhab, A. A novel hybrid load forecasting framework with intelligent feature engineering and optimization algorithm in smart grid. *Appl. Energy* **2021**, *299*, 117178.
5. Ghulam, H.; Wadud, Z.; Khan, I.U.; Khan, I.; Shafiq, Z.; Usman, M.; Khan, M.U.A. Efficient energy management of IoT-enabled smart homes under price-based demand response program in smart grid. *Sensors* **2020**, *20*, 3155.
6. Mohammad, R.; Fotuhi-Firuzabad, M. Outage management in residential demand response programs. *IEEE Trans. Smart Grid* **2014**, *6*, 1453–1462.
7. Aljohani, T.M.; Ebrahim, A.F.; Mohammed, O.A. Dynamic real-time pricing mechanism for electric vehicles charging considering optimal microgrids energy management system. *IEEE Trans. Ind. Appl.* **2021**, *57*, 5372–5381. [CrossRef]
8. Niloofar, Z.; Vahidinasab, V. An MILP formulation for centralized energy management strategy of microgrids. In Proceedings of the 2016 Smart Grids Conference, Kerman, Iran, 20–21 December 2016; pp. 1–8
9. Hou, X.; Wang, J.; Huang, T.; Wang, T.; Wang, P. Smart home energy management optimization method considering energy storage and electric vehicle. *IEEE Access* **2019**, *7*, 144010–144020. [CrossRef]
10. Nabeeha, Q.; Amin, A.; Jamil, U.; Mahmood, A. Optimization techniques for home energy management: A review. In Proceedings of the 2019 2nd International Conference on Computing, Mathematics and Engineering Technologies (iCoMET), Sukkur, Pakistan, 30–31 January 2019; pp. 1–7.
11. Ahmad, K.T.; Ullah, K.; Hafeez, G.; Khan, I.; Khalid, A.; Shafiq, Z.; Usman, M.; Qazi, A.B. Closed-Loop Elastic Demand Control under Dynamic Pricing Program in Smart Microgrid Using Super Twisting Sliding Mode Controller. *Sensors* **2020**, *20*, 4376.

12. Jan, F.; Shah, I.; Ali, S. Short-Term Electricity Prices Forecasting Using Functional Time Series Analysis. *Energies* **2022**, *15*, 3423. [CrossRef]

13. Ismail, S.; Akbar, S.; Saba, T.; Ali, S.; Rehman, A. Short-term forecasting for the electricity spot prices with extreme values treatment. *IEEE Access* **2021**, *9*, 105451–105462.

14. Zheng, C.; An, Y.; Wang, Z.; Wu, H.; Qin, X.; Eynard, B.; Zhang, Y. Hybrid offline programming method for robotic welding systems. *Robot. Comput. Integr. Manuf.* **2022**, *73*, 102238. [CrossRef]

15. Zheng, W.; Xun, Y.; Wu, X.; Deng, Z.; Chen, X.; Sui, Y. A Comparative Study of Class Rebalancing Methods for Security Bug Report Classification. *Sci. Total Environ.* **2021**, *778*, 146312. [CrossRef]

16. Peng, Y.; Xu, Z.; Wang, M.; Li, Z.; Peng, J.; Luo, J.; Xie, S.; Pu, H.; Yang, Z. Investigation of frequency-up conversion effect on the performance improvement of stack-based piezoelectric generators. *Renew. Energy* **2021**, *172*, 551–563. [CrossRef]

17. Yang, S.; Tan, J.; Chen, B. Robust Spike-Based Continual Meta-Learning Improved by Restricted Minimum Error Entropy Criterion. *Entropy* **2022**, *24*, 455. [CrossRef] [PubMed]

18. Zheng, W.; Xun, Y.; Wu, X.; Deng, Z.; Chen, X.; Sui, Y. A Comparative Study of Class Rebalancing Methods for Security Bug Report Classification. *IEEE Trans. Reliab.* **2021**, *70*, 1–13. [CrossRef]

19. Quan, Q.; Gao, S.; Shang, Y.; Wang, B. Assessment of the sustainability of Gymnocypris eckloni habitat under river damming in the source region of the Yellow River. *Sci. Total Environ.* **2021**, *778*, 146312. [CrossRef]

20. Zhou, H.; Xu, C.; Lu, C.; Jiang, X.; Zhang, Z.; Wang, J.; Wang, L. Investigation of transient magnetoelectric response of magnetostrictive/piezoelectric composite applicable for lightning current sensing. *Sens. Actuators A* **2021**, *329*, 112789. [CrossRef]

21. Lu, C.; Zhu, R.; Yu, F.; Jiang, X.; Liu, Z.; Dong, L.; Ou, Z. Gear rotational speed sensor based on FeCoSiB/Pb(Zr,Ti)O3 magnetoelectric composite. *Measurement* **2021**, *168*, 108409. [CrossRef]

22. Liu, S.; Liu, C.; Song, Z.; Dong, Z.; Huang, Y. Candidate Modulation Patterns Solution for Five-Phase PMSM Drive System. *IEEE Trans. Transp. Electrif.* **2021**, *8*, 1194–1208. [CrossRef]

23. Liu, C.; Wu, D.; Li, Y.; Du, Y. Large-scale pavement roughness measurements with vehicle crowdsourced data using semi-supervised learning. *Transp. Res. Part C* **2021**, *125*, 103048. [CrossRef]

24. Li, Y.; Che, P.; Liu, C.; Wu, D.; Du, Y. Cross-scene pavement distress detection by a novel transfer learning framework. *Comput.-Aided Civ. Infrastruct. Eng.* **2021**, *36*, 1398–1415. [CrossRef]

25. Du, Y.; Qin, B.; Zhao, C.; Zhu, Y.; Cao, J.; Ji, Y. A Novel Spatio-Temporal Synchronization Method of Roadside Asynchronous MMW Radar-Camera for Sensor Fusion. *IEEE Trans. Intell. Transp. Syst.* **2021**, 1–12. [CrossRef]

26. Xie, X.; Chen, D. Data-driven dynamic harmonic model for modern household appliances. *Appl. Energy* **2022**, *312*, 118759. [CrossRef]

27. Li, H.; Zhang, Y.; Tai, Y.; Zhu, X.; Qi, X.; Zhou, L.; Lan, H. Flexible transparent electromagnetic interference shielding films with silver mesh fabricated using electric-field-driven microscale 3D printing. *Opt. Laser Technol.* **2022**, *148*, 107717. [CrossRef]

28. Shang, L.; Dong, X.; Liu, C.; He, W. Modelling and Analysis of Electromagnetic Time Scale Voltage Variation Affected by Power Electronic Interfaced Voltage Regulatory Devices. *IEEE Trans. Power Syst.* **2022**, *37*, 1102–1112. [CrossRef]

29. Liu, L.; Meng, X.; Miao, Z.; Zhou, S. Design of a novel thermoelectric module based on application stability and power generation. *Case Stud. Therm. Eng.* **2022**, *31*, 101836. [CrossRef]

30. Pal, S.; Thakur, S.; Kumar, R.; Panigrahi, B. A strategical game theoretic based demand response model for residential consumers in a fair environment. *Int. J. Electr. Power Energy Syst.* **2018**, *97*, 201–210. [CrossRef]

31. Thomas, D.; Deblecker, O.; Ioakimidis, C.S. Optimal operation of an energy management system for a grid-connected smart building considering photovoltaics' uncertainty and stochastic electric vehicles' driving schedule. *Appl. Energy* **2018**, *210*, 1188–1206. [CrossRef]

32. Melhem, F.Y. Optimization Methods and Energy Management in Smart Grids. Ph.D. Thesis, Université Bourgogne Franche-Comté, Bourgogne Franche-Comté, France, 2018.

33. Giaouris, D.; Papadopoulos, A.I.; Seferlis, P.; Papadopoulou, S.; Voutetakis, S.; Stergiopoulos, F.; Elmasides, C. Optimum energy management in smart grids based on power pinch analysis. *Chem. Eng.* **2014**, *39*. [CrossRef]

34. Zafar, R.; Mahmood, A.; Razzaq, S.; Ali, W.; Naeem, U.; Shehzad, K. Prosumer based energy management and sharing in smart grid. *Renew. Sustain. Energy Rev.* **2018**, *82*, 1675–1684. [CrossRef]

35. Angelis, D.; Francesco; Boaro, M.; Fuselli, D.; Squartini, S.; Piazza, F.; Wei, Q. Optimal home energy management under dynamic electrical and thermal constraints. *IEEE Trans. Ind. Inform.* **2012**, *9*, 1518–1527. [CrossRef]

36. Cao, B.; Zhang, Y.; Zhao, J.; Liu, X.; Skonieczny, L.; Lv, Z. Recommendation Based on Large-Scale Many-Objective Optimization for the Intelligent Internet of Things System. *IEEE Internet Things J.* **2021**, 1. [CrossRef]

37. Zhang, L.; Zheng, H.; Cai, G.; Zhang, Z.; Wang, X.; Koh, L.H. Power-frequency oscillation suppression algorithm for AC microgrid with multiple virtual synchronous generators based on fuzzy inference system. *IET Renew. Power Gener.* **2022**. [CrossRef]

38. Yu, D.; Ma, Z.; Wang, R. Efficient Smart Grid Load Balancing via Fog and Cloud Computing. *Math. Probl. Eng.* **2022**. [CrossRef]

39. Yu, D.; Wu, J.; Wang, W.; Gu, B. Optimal performance of hybrid energy system in the presence of electrical and heat storage systems under uncertainties using stochastic p-robust optimization technique. *Sustain. Cities Soc.* **2022**, *83*, 103935. [CrossRef]

40. Zhong, C.; Li, H.; Zhou, Y.; Lv, Y.; Chen, J.; Li, Y. Virtual synchronous generator of PV generation without energy storage for frequency support in autonomous microgrid. *Int. J. Electr. Power Energy Syst.* **2022**, *134*, 107343. [CrossRef]

41. Li, J.; Wang, F.; He, Y. Electric Vehicle Routing Problem with Battery Swapping Considering Energy Consumption and Carbon Emissions. *Sustainability* **2020**, *12*, 10537. [CrossRef]

42. Li, H.; Hou, K.; Xu, X.; Jia, H.; Zhu, L.; Mu, Y. Probabilistic energy flow calculation for regional integrated energy system considering cross-system failures. *Appl. Energy* **2022**, *308*, 118326. [CrossRef]

43. Xu, X.; Niu, D.; Xiao, B.; Guo, X.; Zhang, L.; Wang, K. Policy analysis for grid parity of wind power generation in China. *Energy Policy* **2020**, *138*, 111225. [CrossRef]

44. Bingham, R.D.; Agelin-Chaab, M.; Rosen, M.A. Whole building optimization of a residential home with pv and battery storage in the Bahamas. *Renew. Energy* **2019**, *132*, 1088–1103. [CrossRef]

45. Shakeri, M.; Shayestegan, M.; Reza, S.S.; Yahya, I.; Bais, B.; Akhtaruzzaman, M.; Sopian, K.; Amin, N. Implementation of a novel home energy management system (hems) architecture with solar photovoltaic system as supplementary source. *Renew. Energy* **2018**, *125*, 108–120. [CrossRef]

46. Nemati, M.; Braun, M.; Tenbohlen, S. Optimization of unit commitment and economic dispatch in microgrids based on genetic algorithm and mixed integer linear programming. *Appl. Energy* **2018**, *210*, 944–963. [CrossRef]

47. Nathali, S.B.; Han, K. Mutation operator integrated ant colony optimization based domestic appliance scheduling for lucrative demand side management. *Future Gener. Comput. Syst.* **2019**, *100*, 557–568.

48. Albogamy, F.R.; Khan, S.A.; Hafeez, G.; Murawwat, S.; Khan, S.; Haider, S.I.; Basit, A.; Thoben, K.D. Real-Time Energy Management and Load Scheduling with Renewable Energy Integration in Smart Grid. *Sustainability* **2022**, *14*, 1792. [CrossRef]

49. Sayed, E.; Tantawy, F.; Amer, G.M.; Fayez, H.M. Scheduling home appliances with integration of hybrid energy sources using intelligent algorithms. *Ain Shams Eng. J.* **2022**, *13*, 101676.

50. Ayub, S.; Ayob, S.M.; Tan, C.W.; Ayub, L.; Bukar, A.L. Optimal residence energy management with time and device-based preferences using an enhanced binary grey wolf optimization algorithm. *Sustain. Energy Technol. Assess.* **2020**, *41*, 100798. [CrossRef]

51. Hafeez, G.; Islam, N.; Ali, A.; Ahmad, S.; Usman, M.; Alimgeer, K.S. A modular framework for optimal load scheduling under price-based demand response scheme in smart grid. *Processes* **2019**, *7*, 499. [CrossRef]

52. Campagna, N.; Caruso, M.; Castiglia, V.; Miceli, R.; Viola, F. Energy Management Concepts for the Evolution of Smart Grids. In Proceedings of the 2020 8th International Conference on Smart Grid (icSmartGrid), Sarawak, Malaysia, 4–7 October 2020; pp. 208–213.

53. Liu, Y.; Yang, C.; Jiang, L.; Xie, S.; Zhang, Y. Intelligent edge computing for IoT-based energy management in smart cities. *IEEE Netw.* **2019**, *33*, 111–117. [CrossRef]

54. Hossein, S.A.; Maghouli, P. Energy management of smart homes equipped with energy storage systems considering the PAR index based on real-time pricing. *Sustain. Cities Soc.* **2019**, *45*, 579–587.

55. Choi, J.S. A hierarchical distributed energy management agent framework for smart homes, grids, and cities. *IEEE Commun. Mag.* **2019**, *57*, 113–119. [CrossRef]

56. Yi, D.; Xie, D.; Hui, H.; Xu, Y.; Siano, P. Game-Theoretic Demand Side Management of Thermostatically Controlled Loads for Smoothing Tie-line Power of Microgrids. *IEEE Trans. Power Syst.* **2021**, *36*, 4089–4101

57. Hassan, C.A.; Iqbal, J.; Ayub, N.; Hussain, S.; Alroobaea, R.; Ullah, S.S. Smart Grid Energy Optimization and Scheduling Appliances Priority for Residential Buildings through Meta-Heuristic Hybrid Approaches. *Energies* **2022**, *15*, 1752. [CrossRef]

58. Longe, O.M.; Ouahada, K.; Rimer, S.; Harutyunyan, A.N.; Ferreira, H.C. Distributed Demand Side Management with Battery Storage for Smart Home Energy Scheduling. *Sustainability* **2017**, *9*, 120. [CrossRef]

59. Sajjad, A.; Khan, I.; Jan, S.; Hafeez, G. An Optimization Based Power Usage Scheduling Strategy Using Photovoltaic-Battery System for Demand-Side Management in Smart Grid. *Energies* **2021**, *14*, 2201.

60. Furquan, N.; Aftab, M.A.; Hussain, S.M.; Ali, I.; Tiwari, P.K.; Goswami, A.K.; Ustun, T.S. Virtual power plant management in smart grids with XMPP based IEC 61850 communication. *Energies* **2019**, *12*, 2398.

61. Chengcheng, Z.; Chen, J.; He, J.; Cheng, P. Privacy-preserving consensus-based energy management in smart grids. *IEEE Trans. Signal Process.* **2018**, *66*, 6162–6176.

62. Saeid, T.S.; Seyedshenava, S.; Mohadesi, V.; Esmaeilzadeh, R. Improving Operation Indices of a microgrid by Battery Energy Storage Using Multi Objective Cuckoo Search Algorithm. *Int. J. Electr. Eng. Inform.* **2021**, *13*, 132–151.

63. Juntao, C.; Zhu, Q. A Stackelberg game approach for two-level distributed energy management in smart grids. *IEEE Trans. Smart Grid* **2017**, *9*, 6554–6565.

64. Kevin, F.; Ahrens, M.; Bao, K.; Mauser, I.; Schmeck, H. Towards the modeling of flexibility using artificial neural networks in energy management and smart grids: Note. In Proceedings of the 9th International Conference on Future Energy Systems, Karlsruhe, Germany, 12–15 June 2018; pp. 85–90.

65. Sudip, M.; Mondal, A.; Banik, S.; Khatua, M.; Bera, S.; Obaidat, M.S. Residential energy management in smart grid: A Markov decision process-based approach. In Proceedings of the 2013 IEEE International Conference on Green Computing and Communications and IEEE Internet of things and IEEE Cyber, Physical and Social Computing, Beijing, China, 20–23 August 2013; pp. 1152–1157.

66. Iván, A.; Pena, R.; Blasco-Gimenez, R.; Riedemann, J.; Jara, W.; Pesce, C. An Active/Reactive Power Control Strategy for Renewable Generation Systems. *Electronics* **2021**, *10*, 1061.

67. El-Zonkoly, A.M. Optimal energy management in smart grids including different types of aggregated flexible loads. *J. Energy Eng.* **2019**, *145*, 04019015. [CrossRef]

68. Zhang, L.; Wang, X.; Zhang, Z.; Cui, Y.; Ling, L.; Cai, G. An Adaptive Control Strategy for Interfacing Converter of Hybrid Microgrid Based on Improved Virtual Synchronous Generator. *IET Renew. Power Gener.* **2021**, *16*, 261–273. [CrossRef]

69. Liu, S.; Liu, C.; Huang, Y.; Xiao, Y. Direct Modulation Pattern Control for Dual Three-Phase PMSM Drive System. *IEEE Trans. Ind. Electron.* **2022**, *69*, 110–120. [CrossRef]

70. Gong, X.; Wang, L.; Mou, Y.; Wang, H.; Wei, X.; Zheng, W.; Yin, L. Improved Four-channel PBTDPA Control Strategy Using Force Feedback Bilateral Teleoperation System. *Int. J. Control.* **2022**, *20*, 1002–1017. [CrossRef]

71. Wang, J.; Tian, J.; Zhang, X.; Yang, B.; Liu, S.; Yin, L.; Zheng, W. Control of Time Delay Force Feedback Teleoperation System with Finite Time Convergence. *Front. Neurorobotics* **2022**, *16*, 877069. [CrossRef]

72. Wang, H.; Wu, X.; Zheng, X.; Yuan, X. Virtual Voltage Vector Based Model Predictive Control for a Nine-Phase Open-End Winding PMSM With a Common DC Bus. *IEEE Trans. Ind. Electron.* **2022**, *69*, 5386–5397. [CrossRef]

73. Wang, H.; Zheng, X.; Yuan, X.; Wu, X. Low-Complexity Model Predictive Control for a Nine-Phase Open-End Winding PMSM With Dead-Time Compensation. *IEEE Trans. Power Electron.* **2022**, *37*, 8895–8908. [CrossRef]

74. Zhang, Y.; Shi, X.; Zhang, H.; Cao, Y.; Terzija, V. Review on deep learning applications in frequency analysis and control of modern power system. *Int. J. Electr. Power Energy Syst.* **2022**, *136*, 107744. [CrossRef]

75. Hu, J.; Ye, C.; Ding, Y.; Tang, J.; Liu, S. A Distributed MPC to Exploit Reactive Power V2G for Real-Time Voltage Regulation in Distribution Networks. *IEEE Trans. Smart Grid* **2021**, *13*, 576–588. [CrossRef]

76. Shang, L.; Dong, X.; Liu, C.; Gong, Z. Fast Grid Frequency and Voltage Control of Battery Energy Storage System Based on the Amplitude-Phase-Locked-Loop. *IEEE Trans. Smart Grid* **2022**, *13*, 941–953. [CrossRef]

77. Xiaojun, L.; Zhongbing, Y. Design of Smart Car Control System Based on Camera. *Acta Electron. Malays.* **2017**, *1*, 12–14. [CrossRef]

78. Min-fan, H.; Zhang, F.; Huang, Y.; Chen, J.; Wang, J.; Wang, R. A distributed demand side energy management algorithm for smart grid. *Energies* **2019**, *12*, 426.

79. Subha, S.; Nagalakshmi, S. Design of ANFIS controller for intelligent energy management in smart grid applications. *J. Ambient. Intell. Humaniz. Comput.* **2020**, *12*, 6117–6127. [CrossRef]

80. Xiaowen, X.; Xie, L.; Meng, H. Cooperative energy management optimization based on distributed MPC in grid-connected microgrids community. *Int. J. Electr. Power Energy Syst.* **2019**, *107*, 186–199.

81. Dongmei, Y.; Lu, Z.; Zhang, J.; Li, X. A hybrid prediction-based microgrid energy management strategy considering demand-side response and data interruption. *Int. J. Electr. Power Energy Syst.* **2019**, *113*, 139–153.

82. Ahmed, O.; Achour, Y.; Zejli, D.; Dagdougui, H. Supervisory model predictive control for optimal energy management of networked smart greenhouses integrated microgrid. *IEEE Trans. Autom. Sci. Eng.* **2019**, *17*, 117–128.

83. Mbungu, N.T.; Bansal, R.C.; Naidoo, R.M.; Bettayeb, M.; Siti, M.W.; Bipath, M. A dynamic energy management system using smart metering. *Appl. Energy* **2020**, *280*, 115990. [CrossRef]

84. Albogamy, F.R.; Hafeez, G.; Khan, I.; Khan, S.; Alkhammash, H.I.; Ali, F.; Rukh, G. Efficient Energy Optimization Day-Ahead Energy Forecasting in Smart Grid Considering Demand Response and Microgrids. *Sustainability* **2021**, *13*, 11429. [CrossRef]

85. Hafeez, G.; Alimgeer, K.S.; Wadud, Z.; Shafiq, Z.; Ali, M.U.; Khan, I.; Khan, F.A.; Derhab, A. A Novel Accurate and Fast Converging Deep Learning based Model for Electrical Energy Consumption Forecasting in Smart Grid. *Energies* **2020**, *13*, 2244. [CrossRef]

86. Hafeez, G.; Alimgeer, K.S.; Qazi, A.B.; Khan, I.; Usman, M.; Khan, F.A.; Wadud, Z. A Hybrid Approach for Energy Consumption Forecasting with a New Feature Engineering and Optimization Framework in Smart Grid. *IEEE Access*, **2020**, *8*, 96210–96226. [CrossRef]

87. Chang, G.; Lu, H.; Chang, Y.; Lee, Y. An improved neural network-based approach for short-term wind speed and power forecast. *Renew. Energy* **2017**, *105*, 301–311. [CrossRef]

88. Shirazi, E.; Jadid, S. Optimal residential appliance scheduling under dynamic pricing scheme via hemdas. *Energy Build.* **2015**, *93*, 40–49. [CrossRef]

89. Vergara-Fernandez, L.; Aguayo, M.M.; Moran, L.; Obreque, C. A MILP-based operational decision-making methodology for demand-side management applied to desalinated water supply systems supported by a solar photovoltaic plant: A case study in agricultural industry. *J. Clean. Prod.* **2022**, *334*, 130123. [CrossRef]